AoI Analysis of RIS-Assisted Vehicular Networks and the Impact on Cooperative Maneuvers

Suleman Munawar[1], Ehizogie I. Emoyon-Iredia[2,3], Hassaan Khaliq Qureshi[1], Chrysostomos Chrysostomou[2,3], Nikolaos Ntetsikas[2,3], Christos Liaskos[4,5], and Marios Lestas[2,3]

[1]National University of Sciences and Technology (NUST), Islamabad, Pakistan.
[2]Frederick Research Center, Nicosia, Cyprus.
[3]Frederick University, Nicosia, Cyprus.
[4]University of Ioannina, Department of Computer Science Engineering, Greece.
[5]Foundation for Research and Technology (FORTH), Greece.
[1]smunawar.mscse23ssines@student.nust.edu.pk, hassaan.khaliq@seecs.edu.pk
[2,3]{st015229, st023422}@stud.frederick.ac.cy, {ch.chrysostomou, eng.lm}@frederick.ac.cy
[4,5]cliaskos@ics.forth.gr

***Abstract*—Cooperative, Connected, and Automated Mobility (CCAM) is based on fast, secure, and reliable Vehicle-to-Everything (V2X) communication to enable collective perception and maneuver coordination in autonomous driving. However, high-frequency wireless communication, particularly in the millimeter wave (mmWave) and terahertz (THz) bands, is highly susceptible to environmental obstacles, leading to severe signal attenuation and communication delays. This study investigates the integration of Reconfigurable Intelligent Surfaces (RIS) into vehicular networks to mitigate these challenges and analyzes their impact on Age of Information (AoI) and Peak AoI (PAoI) metrics. The latter metrics are highly relevant to feedback delays introduced in the Cooperative Control Schemes of Autonomous Vehicles, which are well known to compromise their stability. Their characterization is thus crucial for the performance assessment of the automatic controllers with this characterization in the presence of RIS not investigated as of now in the literature. Using the All-or-Nothing Receiver Model (ANRM) and Distance-Dependent Propagation Model (DDPM), we extend AoI formulations by incorporating RIS path loss characteristics revealing that RIS-assisted networks significantly reduce AoI and PAoI values, enabling reliable cooperative control in vehicular systems. We consider a cooperative merging maneuver on an intersection as our test case and demonstrate that the effect of the introduced delays on the cooperative control scheme performance is minimal. Passive RISs are assumed throughout the study, due to their energy efficient operation as compared to active metasurfaces.**

***Index Terms*—Cooperative Autonomous Mobility, Vehicle-to-Everything (V2X), Age of Information (AoI), Reconfigurable Intelligent Surfaces (RIS), Path Loss Models, Vehicular Communication, Communication Delays, Cooperative Control, Merging Maneuver.**

I. Introduction

The development of autonomous vehicle (AV) technology is revolutionizing the transportation sector, with the promise of increased safety, efficiency, and sustainability. Autonomous vehicles are expected to minimize human error, reduce congestion, and optimize fuel consumption, making them a cornerstone of future smart cities. To achieve this, AVs rely on a synergy of advanced technologies, including sensors for environmental perception, artificial intelligence for decision-making, and wireless communication systems for real-time data exchange [1], [2]. Among these, reliable and low-latency vehicular communication systems are paramount, enabling vehicles to share critical information about traffic, road conditions, and navigation in Vehicle-to-Everything (V2X) scenarios [3].

Cooperative, Connected, and Automated Mobility (CCAM) is transforming the transportation industry by enhancing road safety, traffic efficiency, and vehicle coordination. A crucial component of this transformation is the integration of V2X communication, which enables vehicles to share real-time information about their surroundings through Collective Awareness Messages (CAM), Collective Perception Messages (CPM), and Maneuver Coordination Messages (MCM) [4]. This exchange of information is fundamental for cooperative driving, allowing vehicles to navigate complex scenarios such as merging, lane changing, and intersection management [5].

High-frequency communication, particularly in the millimeter wave (mmWave) and terahertz (THz) bands, offers significant advantages for V2X systems due to higher bandwidth and lower latency. However, these frequencies are more susceptible to obstacles, path loss, and environmental attenuation, making reliable communication a significant challenge [6], [7], [8] and in urban environments, buildings, vehicles, and foliage frequently obstruct line-of-sight (LoS) links, while adverse weather conditions further degrade signal quality. These disruptions can compromise the effectiveness of cooperative perception and maneuver coordination, impacting the stability and safety of autonomous driving systems [9], [10]. A promising solution to these challenges is the use of Reconfigurable Intelligent Surfaces (RIS), a revolutionary technology capable of dynamically manipulating electromagnetic waves to create alternative propagation paths, bypass obstacles, and enhance signal strength [11], [12]. While RIS technology has been

extensively studied for physical layer optimizations, its impact on end-to-end vehicular network performance and cooperative control schemes remains largely unexplored [13].

A key issue in vehicular networks is communication delays, which can adversarially affect cooperative control algorithms. Cooperative driving relies on feedback control loops, where each vehicle makes real-time decisions based on received information. Delays in these feedback loops are well known to compromise stability margins and degrade performance, rendering their characterization and minimization crucial for safe and efficient autonomous operation. Despite the critical role of delays in cooperative driving systems, and the rich literature in their analysis, we do note a gap in the literature in control theoretic delay analysis based on realistic communication/network theoretic delay characterizations [14]. Particularly, in the context of RIS-assisted vehicular communications, such an analysis is absent in the literature, despite Age of Information (AoI) analysis in RIS enabled systems in other domains [15].

As such, this study addresses this research gap by integrating RIS-assisted communication models into the AoI framework, analyzing how RIS influences the freshness of information in vehicular networks and thus the associated delays. Passive RISs are considered due to energy efficient operation compared to actives metasurfaces. The research specifically examines single-RIS and dual-RIS configurations, evaluating their impact on AoI, Peak AoI (PAoI), and cooperative driving maneuvers. A key focus is to determine whether RIS-assisted paths introduce communication delays that could affect vehicle coordination and stability. To this end, a cooperative merging maneuver is considered, assessing the impact of RIS-induced delays on autonomous vehicle performance.

The primary contributions of this paper are:

- Integration of RIS-assisted propagation models into AoI and PAoI frameworks using established models.
- Analysis of RIS performance under different configurations, including single and dual-RIS setups.
- Evaluation of the effect of RIS-assisted paths on communication delays, particularly in the context of cooperative driving maneuvers.

By bridging the gap between theoretical path loss models and real-time vehicular control systems, this study provides critical insights into the feasibility of RIS deployment in autonomous driving. The findings contribute to the broader goal of enhancing the robustness and reliability of V2X communication in high-frequency vehicular networks.

II. Mathematical Formulation

In this section, we present the mathematical framework adopted in our work. Specifically, we incorporate the path loss model of [16] and evaluate the performance gains of RIS integration, using the AoI and PAoI metrics, drawn from the All-or-Nothing Receiver Model (ANRM) and the Distance-Dependent Propagation Model (DDPM) of [17].

A. Path loss Model of RIS-Assisted Networks

The base path loss model is adopted from [16], where the received power in a multi-hop RIS-assisted network, is given by:

$$P_r = \frac{P_t G_t G_r \prod_{i=1}^{N_{RIS}} G_i^{RIS}}{\left(\frac{4\pi f^2}{c}\right)^2 \left(\sum_{i=1}^{N_{RIS+1}} d_i\right)^{\alpha}} \tag{1}$$

where P_t, G_t, and G_r represent the transmission power, the transmitter antenna gain, and the receiver antenna gain, respectively, f is the frequency and c is the speed of light. N_{RIS} is the number of RISs, with N_{RIS+1} indicating the number of hops along the full path. G_i^{RIS} represents the gain of the ith hop of the path and α is the path loss exponent. The RIS gain is given by [16]:

$$\mathbf{G} = \mathbf{P}\frac{2\pi}{(\mathbf{P}^T \cdot \mathbf{1})^T \cdot A(\theta, d_\theta, d_\phi)} \tag{2}$$

where $\mathbf{P}$ is the transmitted power towards the receiver and $A(\theta, d_\theta, d_\phi)$ is the area of a unit spherical element of elevation θ and elevation and azimuth angular resolutions d_θ and d_ϕ, respectively. These are given by:

$$\begin{aligned}\Phi_{m,n} = \frac{2\pi d_u}{\lambda}[&n(\cos(\phi_r)\sin(\theta_r) - \cos(\phi_i)\sin(\theta_i)) \\ &+m(\sin(\phi_r)\sin(\theta_r) - \sin(\phi_i)\sin(\theta_i))]\end{aligned} \tag{3}$$

$$\begin{aligned}\Theta_{m,n} = \frac{2\pi d_u}{\lambda}[&n(-\cos(\phi_r x)\sin(\theta_r x) + \cos(\phi_t x)\sin(\theta_t x)) \\ &+m(-\sin(\phi_r x)\sin(\theta_r x) + \sin(\phi_t x)\sin(\theta_t x))]\end{aligned} \tag{4}$$

$$\mathbf{P}_{\phi_{rx},\theta_{rx}} = \left|\sum_{m=0}^{M_r-1}\sum_{n=0}^{N_r-1} f(\phi_{tx},\theta_{tx}) f(\phi_{rx},\theta_{rx}) a_{m,n} e^{-j(\Phi_{m,n}+\Theta_{m,n})}\right|^2, \quad \forall(\phi_{rx},\theta_{rx}) \tag{5}$$

$$A(\theta, d_\theta, d_\phi) = \begin{cases} d_\phi\left(1 - \cos\left(\frac{d_\theta}{2}\right)\right), & \text{if } \theta = 0, \\ d_\phi\left(\cos\left(\theta - \frac{d_\theta}{2}\right) - \cos\left(\theta + \frac{d_\theta}{2}\right)\right), & \text{if } 0 < \theta < \frac{\pi}{2}, \\ d_\phi \cos\left(\theta - \frac{d_\theta}{2}\right), & \text{if } \theta = \frac{\pi}{2}. \end{cases} \tag{6}$$

where (3) and (4) correspond to the phase shifts of the reflective elements indexed by (m, n) in the RIS position matrix, and d_u is the inter element distance given by $d_u = \frac{\lambda}{p_\lambda}$, with λ indicating the wavelength and p_λ the number of elements per wavelength. ϕ and θ are azimuth and elevation angles, respectively. Different subscripts indicate incidence (i), reflection (r), transmitter (tx), and receiver (rx) angles. Moreover, (5) denotes the power emitted towards receivers direction (ϕ_{rx}, θ_{rx}). (6) is the area of the spherical element of a unit sphere for elevation θ and for elevation and azimuth angular resolutions d_θ and d_ϕ.

B. Age of Information (AoI) and Peak AoI (PAoI)

The AoI models are derived from [17], with AoI measuring the freshness of information evaluated as the time elapsed

since the most recent packet was generated. Two models are considered, namely the ANRM and the DDPM.

1) All-or-Nothing Receiver Model: This model leverages a number of simplified assumptions to provides a tractable framework for analyzing AoI in semi-persistent scheduling systems. It assumes that a message transmitted without collision is always successfully decoded, while collisions lead to complete loss of the message. The ANRM model evaluates PAoI and average AoI using the following equations:

$$E[PAoI] = \frac{1}{p_s} \tag{7}$$

$$E[AoI] = \frac{1}{2} + \frac{(1-p_s)^2}{p_s(1-p_{11})} \tag{8}$$

where p_s is the success probability and p_{11} is the transition probability to maintain successful transmission.

2) Distance-Dependent Propagation Model: This model is an extension of the previous model to capture the effects of distance-based propagation and fading. The DDPM model evaluates the probability of success p_s^{DDPM} taking into account distance-dependent path loss and interference [17]:

$$p_s^{DDPM} = e^{-\frac{\gamma}{S(x)}} \sum_{n=1}^{N} \frac{Kn\tilde{\pi}_n}{N} \exp\left(-\frac{2(n-1)x\gamma^{1/\alpha}\pi/\alpha}{L\sin(\pi/\alpha)}\right) \tag{9}$$

where γ is the threshold for Signal-to-Noise-plus-Interference Ratio (SNIR), N is the number of nodes, K is the number of sub-channels (SCs), $\tilde{\pi}$ is the stationary probability vector, L is the length of road, x is the distance between the transmitter and the receiver, and α is the path loss exponent. $S(x)$ is the transmission power level normalized to noise power, given by:

$$S(x) = \frac{G_d(x)P_{tx}}{P_{no}} \tag{10}$$

where $G_d(x)$ is the deterministic component of the gain, assumed to follow a power law, x is the distance between the transmitter and the receiver, P_{tx} represents the transmission power level, and P_{no} is the background noise power level.

3) Integration of ANRM and DDPM models: In this research work, we have integrated the ANRM and DDPM models to investigate the effects of distance-based propagation on the AoI and PAoI metrics. For this purpose, we leveraged the AoI and PAoI metrics of ANRM model in eq. (7) and (8) and substituting the p_s of the ANRM model with the p_s^{DDPM} of the DDPM model, given in eq. (9). The modified equations for AoI and PAoI are given as below:

$$E[PAoI] = \frac{1}{p_s^{DDPM}} \tag{11}$$

$$E[AoI] = \frac{1}{2} + \frac{(1-p_s^{DDPM})^2}{p_s^{DDPM}(1-(p_{11} * p_s^{DDPM}))} \tag{12}$$

C. Integration of RIS Path Loss Model with AoI Metrics

To evaluate the impact of RIS-assisted networks on the AoI metrics, we extended the AoI formulation by incorporating the path loss model of RIS networks. This integration allows for the analysis of AoI under configurations with one or more RISs. The integration involves substituting the term $S(x)$ in eq. (9) with the RIS-specific path loss model thus yielding:

$$S^{RIS}(x) = \frac{P_{tx}G_tG_r\prod_{i=1}^{N_{\text{RIS}}} G_i^{\text{RIS}}}{P_{n_0}\left(\frac{4\pi f}{c}\right)^2\left(\sum_{i=1}^{N_{\text{RIS}}+1} d_i\right)^{\alpha}} \tag{13}$$

Using the updated $S(x)$ in eq. (13), the success probability in eq. (9) is then calculated as:

$$p_s^{DDPM} = e^{-\frac{\gamma}{S^{RIS}(x)}} \sum_{n=1}^{N} \frac{Kn\tilde{\pi}_n}{N} \exp\left(-\frac{2(n-1)x\gamma^{1/\alpha}\pi/\alpha}{L\sin(\pi/\alpha)}\right) \tag{14}$$

To account for undesirable amplifications of the power term, $S^{RIS}(x)$ was scaled down by a factor of 10^{-3}. This ensured numerical stability while preserving the relative differences in gains.

III. Simulation Results

For the simulation results, we evaluated the performance of the ANRM and DDPM models, with and without RIS-assisted networks. The simulation parameters are shown in Table I. The first simulation experiments involved the ANRM model without RIS integration to establish a baseline for success probability, AoI, and PAoI metrics with respect to the persistence probability. As shown in Fig. 1, our results align with the theoretical expectations of the original model in [17]. It states that a specific probability of persistence exists for which the AoI's value is minimal.

In the next set of simulation experiments, the DDPM model was leveraged to obtain PAoI and AoI values, using equations (11) and (12), respectively. The distance between the transmitter and the receiver was kept constant as x = 350m with the results depicted in Fig. 2. We observe that, when compared to the ANRM model, the DDPM model exhibits higher AoI values due to the inclusion of path loss and interference effects.

A. RIS integration in the DDPM model

We then evaluate the effect of RIS integration in the DDPM model with reference to the AoI and PAoI metrics. The evaluation involves comparison between the RIS and no RIS cases. A single RIS is first considered. The following values are adopted for the metasurface parameters: $\theta = 45°$, $\phi_{tx} = 0°$, $\theta_{tx} = 0°$, $\phi_{rx} = 45°$, $\theta_{rx} = 45°$, $\phi_i = 45°$, $\phi_r = 45°$, $\theta_i =$

TABLE I: Simulation Parameters

Notation	Description	Value
L	Length of road	800 m
f	Carrier frequency	25 GHz
N	Number of nodes	195
K	Number of SCs per RRI	200
α	Pathloss exponent	2
P_{tx}	Transmission power level	20 dBm
P_{no}	Background noise power level	−98.83 dBm
γ	SNIR threshold	20.27 dB
p_λ	Number of elements per wavelength	5
M_r	Number of elements in each row of RIS	25
N_r	Number of elements in each column of RIS	25
G_t	Transmitter antenna gain	1
G_r	Receiver antenna gain	1
d_θ, d_ϕ	Angular resolutions	1°

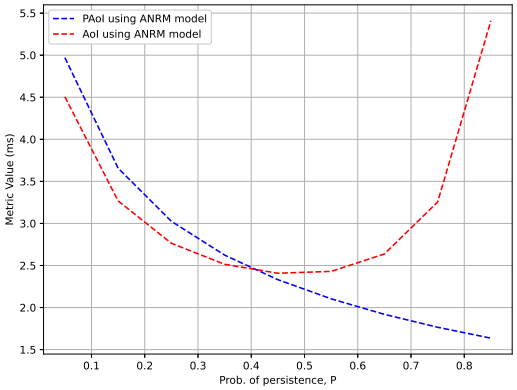

Fig. 1: AoI and PAoI vs. Persistence probability using the ANRM model in [17]

45°, and $\theta_r = 45°$. Similar to the previous case, the distance between the transmitter and the receiver is kept constant at x = 350m with the results depicted in Fig. 3 and Fig. 4. It is evident from Fig. 3, that RIS integration is beneficial in the sense that the success probability is higher. Similarly, Fig. 4 reveals that both AoI and PAoI metrics report consistently lower values, again demonstrating the beneficial effects of RIS integration.

The next set of experiments aim at evaluating the effect of transmitter-receiver distance on the observed performance. Towards this end, the persistence probability was kept constant at $P = 0.5$ with the distance x assuming the values [20m, 70m,

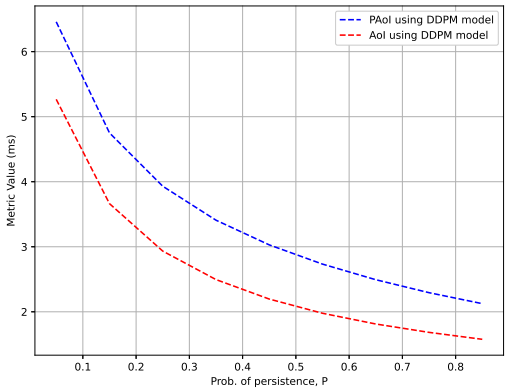

Fig. 2: AoI and PAoI vs. Persistence probability using the DDPM model without RIS-assisted networks

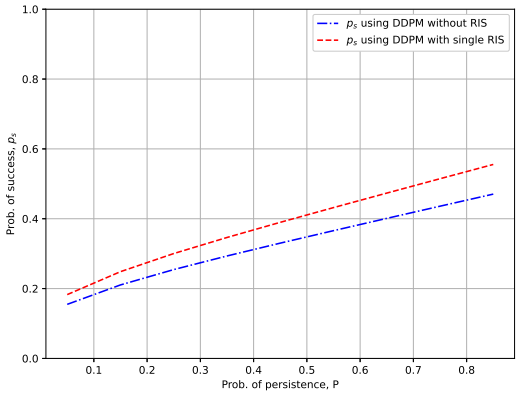

Fig. 3: Success probability vs. Persistence probability of the DDPM framework with and without a single RIS

200m, 350m, 500m, 700m]. In Fig. 5, we observe a sharp deterioration in performance as the distance is increased with the AoI and PAoI abruptly increasing. RIS integration is again observed to be beneficial in the sense that it flattens the rate of increase. This can be attributed to the RIS gain.

1) Two RIS Results: We then consider experiments, which aim at investigating the effect of increasing the number of RISs to two (2). The comparison is made against the single RIS case, which has exhibited consistently superior performance relative to the no-RIS case. The distance is fixed to 350m and the metasurface parameters are chosen as $\theta = 45°$, $\phi_{tx} = 0°$, $\theta_{tx} = 0°$, $\phi_{rx} = 45°$, $\theta_{rx} = 45°$, $\phi_i = [45°, 0°]$, $\phi_r = [0°, 45°]$, $\theta_i = [45°, 0°]$, and $\theta_r = [0°, 45°]$. The results are depicted in Fig. 6 and Fig. 7 demonstrating that multiple RIS integration is beneficial in achieving consistently higher success probability values and lower AoI and PAoI values.

2) Impact of fewer RIS Elements: The next simulation study aims at investigating the effect of changing the meta-surface characteristics on the observed performance. As a case study, we consider changes in the number of elements decreasing the total number of elements to $N = 20$ and $M = 20$

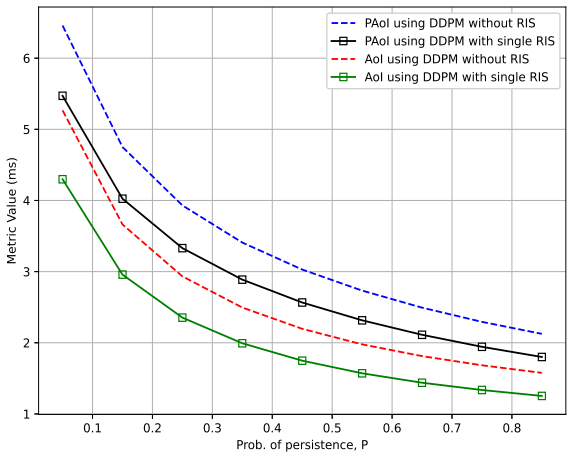

Fig. 4: AoI and PAoI vs. Persistence probability comparison of the DDPM framework with and without a single RIS

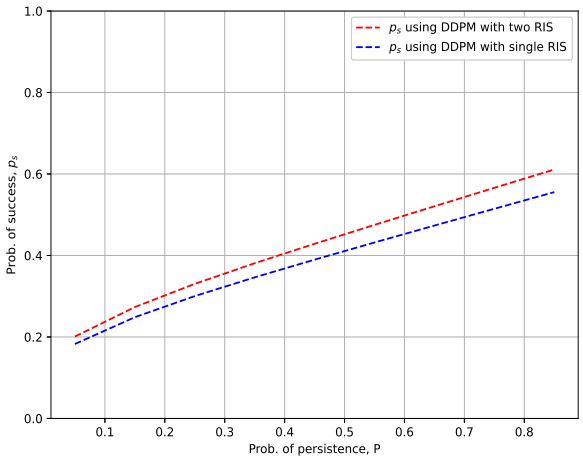

Fig. 6: Success probability vs. Persistence probability comparison of the DDPM framework with single and two RIS

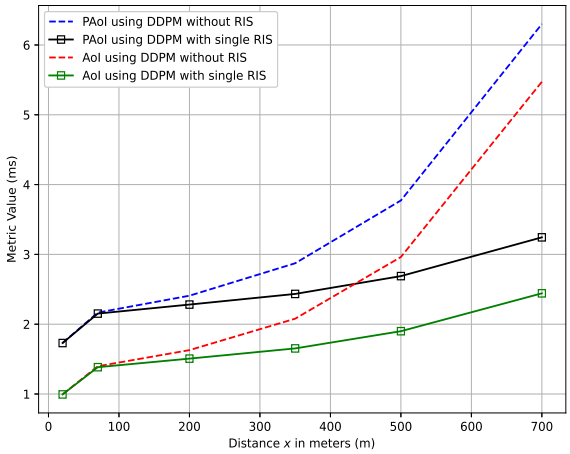

Fig. 5: Comparison of AoI and PAoI vs. distance of the DDPM framework with and without a single RIS

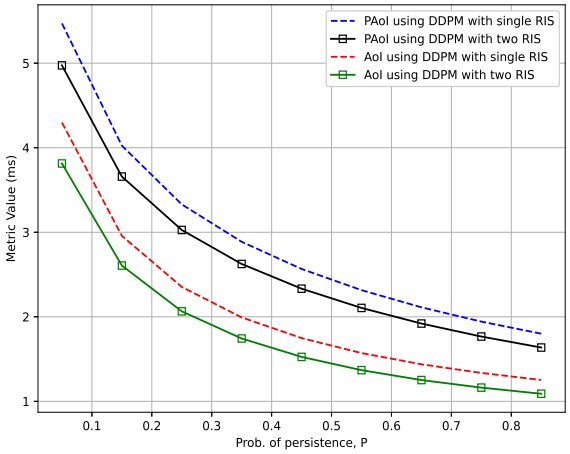

Fig. 7: AoI and PAoI vs. Persistence probability comparison of the DDPM framework with single and two RIS

with the number of elements that can be placed per wavelength fixed to $p_\lambda = 3$. We observe from Fig. 8 and 9 that decreasing the elements results in a deterioration in performance in both the success probability and the AoI and PAoI metrics.

IV. Cooperative Merging Maneuver

The preceding AoI analysis highlights that in the presence of RISs an upper bound of 3ms can be reported on the observed delays. The question that arises is whether such delays can prove sufficient to lead to a significant deterioration of cooperative maneuver performance in the case of Connected and Automated Driving. To investigate the latter, we consider a cooperative merging maneuver on an intersection where vehicle states are exchanged between vehicles via RIS assisted V2X communications. RIS deployment is necessary to counter for obstructions that create Non-Line-of-sight (NLOS) links. The scenario depicted in Fig. 10 involves cooperative autonomous vehicles (CAV), with Platoon C approaching from the south of the intersection attempting to merge into the main traffic flow from left to right. Near the intersection, the RIS is cardinally mounted north-west at a height of about 10 meters. The RIS receives driving state information (DSI) from all vehicles in each platoon, such as position, velocity, acceleration, etc., and uses controllers to commence platoon control decisions.

We aim at letting platoon C merge into the traffic flow without forcing platoon B cars to slow down (i.e., if the merging gap is sufficient). By this, we optimize road throughput and conserve fuel by eliminating unnecessary acceleration. Without loss of generality, we consider platoons made up of two cooperative vehicles identifying the designated leader

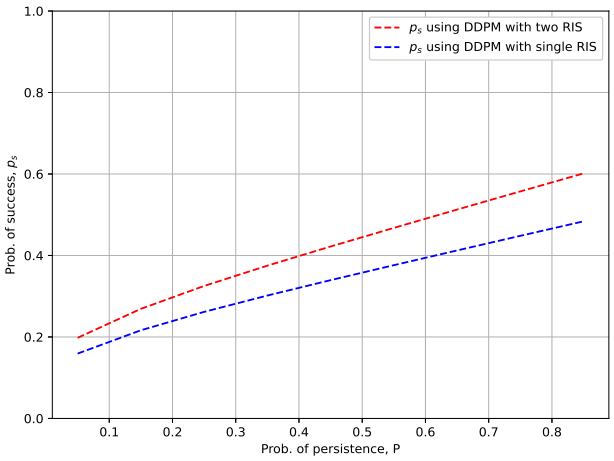

Fig. 8: Success probability vs. Persistence probability comparison of the DDPM framework with single and two RIS with fewer reflective elements

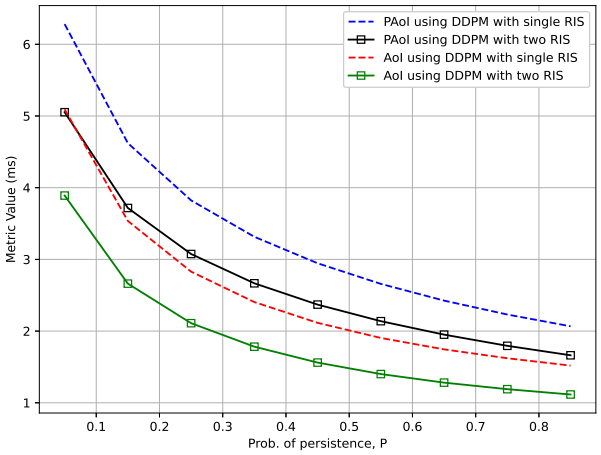

Fig. 9: AoI and PAoI vs. Persistence probability comparison of the DDPM framework with single and two RIS with fewer reflective elements

vehicle as the first car of each platoon and the second car to be the following vehicle. To execute the merging maneuever, the leader vehicle of platoon C must be aware of the position of the following vehicle of platoon A. Platoon B has an unobstructed line of sight (LoS) to platoon A, so the leader of that platoon can share such information using cooperative perception (CP), which we will investigate in a separate work.

To execute the maneuver, we utilize the control laws proposed in [18] introducing time delays to account for the communication delays, as analyzed in the previous sections. The control law accounting for the delays is given below:

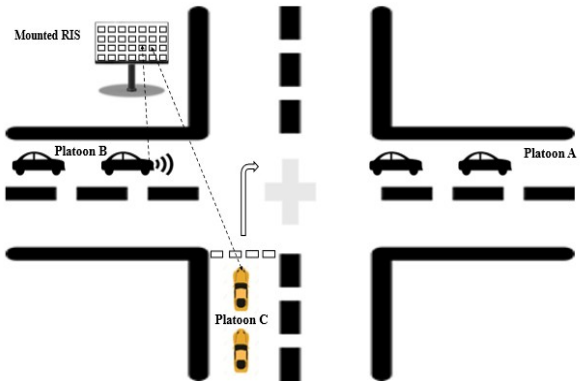

Fig. 10: Cooperative Merging Maneuver

$$u_i'(t) = -\sum_{l=1}^{r_i}\Big[K_{pi}\big(p_i(t-\Delta) - p_{i-l}(t-\Delta)\big) + \sum_{k=i-l+1}^{i}\big(h_k v_k(t-\Delta) + d_k\big) + K_{vi}(t-\Delta)\big(v_i(t-\Delta) - v_{i-l}\big) + K_{ai}(t-\Delta)\big(a_i(t-\Delta) - a_{i-l}\big)\Big] \quad (15)$$

where $r_i \leq i$ denotes the number of the vehicles directly ahead of vehicle i that send their information to it. In a heterogeneous platoon under the MPF topology, each vehicle is allowed to establish communication with a different number of predecessors. The control parameters (k_{pi} , k_{vi} , k_{ai}) are tunable gains for feeding back distance, velocity and acceleration errors between vehicle i and the l-th vehicle ahead of i.

A. Results for RIS enabled Cooperative merging with delays

We show the vehicular movements with and without a time delay of 3ms in Fig. 11. Multiple predecessor following (MPF) is used in both Fig. 11(a) and Fig 11(b), in which predecessors can exchange DSI. The leader vehicle (Vehicle 0) and follower vehicle 1 form platoon A, platoon B comprises the follower vehicles 4 and 5, while platoon C comprises the follower vehicles 2 and 3, as depicted in the legend. Simulations indicate successful execution of the maneuver and minimal differences between the delay and no delay cases. This highlights that communication delays, as these are derived from the AoI analysis do not significantly affect the peformed maneuvers. Follower vehicle 4 becomes the designated leader of platoon B during the merging maneuver into the main traffic flow after 1.2s. Also, speed regulation from controllers take place after 3s, where we can observe drastic changes in vehicular paths. Lastly, we see a successful merging maneuver after 6s with equal inter-vehicular distances. However, the one slightly noticeable but crucial variation we can observe is the time response; where for Fig. 11(a) vehicles 2 and 3 (Platoon C) merge into the main traffic flow with a 0.2s better response than vehicles in Fig 11(b). In both results, a successful merging maneuver occurs without collision, and system stability is maintained.

V. Conclusion

This study investigates the integration of Reconfigurable Intelligent Surfaces (RIS) into vehicular networks to improve

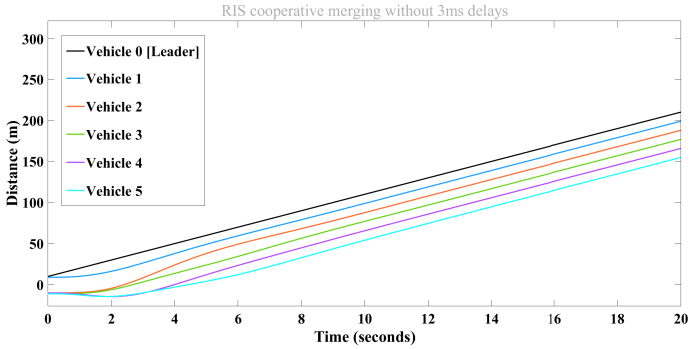

(a)

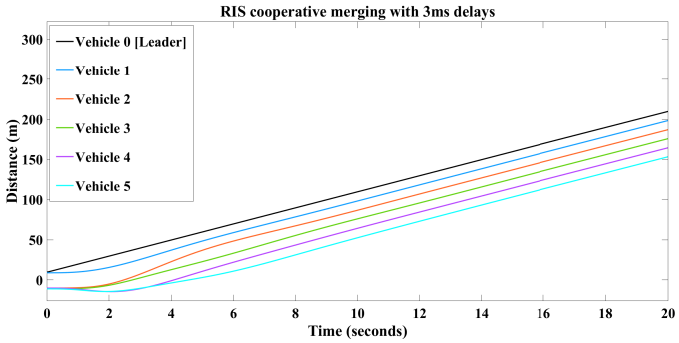

(b)

Fig. 11: RIS enabled cooperative merging a)without b)with 3ms delay

high-frequency communication reliability and evaluates its impact on Age of Information (AoI) and Peak AoI (PAoI) metrics. By incorporating RIS-specific path loss models into the ANRM and DDPM frameworks, the research examines how single and dual-RIS setups influence information freshness and transmission success probability. Simulation results reveal that RIS-assisted networks significantly enhance AoI and PAoI performance by mitigating path loss and reducing the impact of environmental obstructions. Beyond that, the paper harnesses the delay bounds derived from the AoI analysis to investigate their effect on RIS assisted cooperative driving. A platoon merging maneuver is used as a test case highlighting the minimal effect of these delays on the successful execution of the maneuver.

Acknowledgements

This research has received support from the project BRIDGE2HORIZON/0823A/004 (AUTOMETA), which is implemented under the Cohesion Policy Funds "THALIA 2021-2027" with EU co-funding.

References

[1] J. Ma, L. Zhong and R. Onishi, "LEO Satellite Communication Simulation Framework for Connected Vehicles", *GLOBECOM 2023 - 2023 IEEE Global Communications Conference*, Kuala Lumpur, Malaysia, 2023, pp. 6597-6602.

[2] S. Munawar, Z. Ali, M. Waqas, S. Tu, S. A. Hassan and G. Abbas, "Cooperative Computational Offloading in Mobile Edge Computing for Vehicles: A Model-Based DNN Approach", in *IEEE Transactions on Vehicular Technology*, vol. 72, no. 3, pp. 3376-3391, March 2023.

[3] G. Naik, B. Choudhury and J. -M. Park, "IEEE 802.11bd 5G NR V2X: Evolution of Radio Access Technologies for V2X Communications", in *IEEE Access*, vol. 7, pp. 70169-70184, 2019.

[4] M. Klimke, M. B. Mertens, B. Völz, and M. Buchholz, "Towards Cooperative Maneuver Planning in Mixed Traffic at Urban Intersections", arXiv:2403.16478v1, 2024.

[5] M. Rondinone, T. Walter, R. Blokpoel and J. Schindler, "V2X Communications for Infrastructure-Assisted Automated Driving," *2018 IEEE 19th International Symposium on "A World of Wireless, Mobile and Multimedia Networks" (WoWMoM)*, Chania, Greece, 2018, pp. 14-19.

[6] L. Li, W. Zhang, X. Wang, T. Cui and C. Sun, "NLOS Dies Twice: Challenges and Solutions of V2X for Cooperative Perception," in *IEEE Open Journal of Intelligent Transportation Systems*, vol. 5, pp. 774-782, 2024.

[7] N. Moraitis and K. S. Nikita, "Propagation Study in a Dense Urban Environment at the Sub-THz Band for Future Wireless Communications", *2023 17th European Conference on Antennas and Propagation (EuCAP)*, Florence, Italy, 2023, pp. 1-5.

[8] H. M. Rahim, C. Y. Leow, T. A. Rahman, A. Arsad and M. A. Malek, "Foliage attenuation measurement at millimeter wave frequencies in tropical vegetation", *2017 IEEE 13th Malaysia International Conference on Communications (MICC)*, Johor Bahru, Malaysia, 2017, pp. 241-246.

[9] E. Cinque, F. Valentini, A. Persia, S. Chiocchio, F. Santucci and M. Pratesi, "V2X Communication Technologies and Service Requirements for Connected and Autonomous Driving," *2020 AEIT International Conference of Electrical and Electronic Technologies for Automotive (AEIT AUTOMOTIVE)*, Turin, Italy, 2020, pp. 1-6.

[10] S. Dimce, M. S. Amjad and F. Dressler, "mmWave on the Road: Investigating the Weather Impact on 60 GHz V2X Communication Channels", *2021 16th Annual Conference on Wireless On-demand Network Systems and Services Conference (WONS)*, Klosters, Switzerland, 2021, pp. 1-8.

[11] M. Deng et al., "Reconfigurable Intelligent Surfaces Enabled Vehicular Communications: A Comprehensive Survey of Recent Advances and Future Challenges," in *IEEE Transactions on Intelligent Vehicles*, doi: 10.1109/TIV.2024.3476934.

[12] N. Ashraf et al., "Intelligent Beam Steering for Wireless Communication Using Programmable Metasurfaces", in *IEEE Transactions on Intelligent Transportation Systems*, vol. 24, no. 5, pp. 4848-4861, May 2023.

[13] Y. Chen, Y. Wang, J. Zhang, P. Zhang and L. Hanzo, "Reconfigurable Intelligent Surface (RIS)-Aided Vehicular Networks: Their Protocols, Resource Allocation, and Performance," in *IEEE Vehicular Technology Magazine*, vol. 17, no. 2, pp. 26-36, June 2022.

[14] G. Ma, P. R. Pagilla, and S. Darbha, "Benefits of V2V communication in connected and autonomous vehicles in the presence of delays in communicated signals", arXiv:2404.08879v2, 2024.

[15] K. Qi, Q. Wu, P. Fan, N. Cheng, W. Chen, J. Wang, and K. B. Letaief, "Deep-Reinforcement-Learning-Based AoI-Aware Resource Allocation for RIS-Aided IoV Networks", *IEEE Transactions on Vehicular Technology*, Volume 74, 2025.

[16] M. Segata, P. Casari, M. Lestas, A. Papadopoulos, D. Tyrovolas, T. Saeed, G. Karagiannidis, C. Liaskos, "CoopeRIS: A framework for the simulation of reconfigurable intelligent surfaces in cooperative driving environments", *Computer Networks*, Volume 248, 2024, 110443, ISSN 1389-1286.

[17] A. Rolich, I. Turcanu, A. Vinel, A. Baiocchi, "Understanding the impact of persistence and propagation on the Age of Information of broadcast traffic in 5G NR-V2X sidelink communications", in *Computer Networks*, Volume 248, 2024, 110503, ISSN 1389-1286.

[18] Y. Bian, Y. Zheng, W. Ren, S. E. Li, J. Wang, K. Li, "Reducing time headway for platooning of connected vehicles via V2V communication", *Transportation Research Part C: Emerging Technologies*, Volume 102, 2019, ISSN 0968-090X.